Armenian Journal of Physics, 2020, vol. 13, issue 3, pp. 255-262

X-Ray Diffraction Method for Investigation of Imperfections in Crystals Based on Interpretation of Sectional Topogram

H.R. Drmeyan, H.G. Margaryan*

Institute of Applied Problems of Physics NAS of the Republic of Armenia
25 Hrachya Nersissian Str., 0014, Yerevan, Republic of Armenia
*E-mail: drm-henrik@mail.ru

Received 23 June 2020

Abstract: To increase the resolution of X-ray diffraction methods, a new method is proposed in the work, which is theoretically proven and with which thin structures of diffraction images are experimentally observed. The X-ray interference pattern obtained by X-ray diffraction in a system consisting of a two-crystal system with a narrow gap and a thick absorbing crystal was studied. The theoretical period of the interbranch scattered bands obtained from this system is calculated. It is shown that the presence of a thick plate makes it possible to increase the period of the bands by about 5 to 10 times. For the first time, two dynamic effects were simultaneously observed: on one topogram, interbranch scattering bands and moire patterns formed in a two-crystal system were observed.

Keywords: X-ray diffraction, fine structures of X-ray interference patterns, two-crystal system, interbranch band scattering.

1. Introduction

X – ray diffraction methods, which are widely used in detecting structural imperfections in crystalline materials, have limited capabilities due to insufficient resolution, in particular, it is impossible to detect the fine structure of X – ray diffraction patterns or section topograms. The unambiguous interpretation of X – ray topographic images of crystal imperfections is sometimes greatly complicated, on the one hand, due to the overlapping of various dynamic and kinematic effects and their superimposition on imperfections, on the other.

It is known [1–5] that the image of defects depends on the thickness of the crystal, on the divergence and spectral composition of the primary incident beams, on the orientation of the reflecting families of planes relative to the defect, on the location of the defect in the crystal — on the input, output surface, or in the bulk of the crystal and on the degree deformation of the surface layer. The image of imperfections also essentially depends on whether the scattering of X – rays by these defects is kinematic or dynamic. Sometimes an inhomogeneous intensity distribution (splitting into separate components) appears in the diffracted beam, which can be a manifestation of both crystal defects and dynamic scattering effects in perfect crystals.

A number of works [6–9] have been devoted to X – ray studies of the influence of these factors on the intensity of scattering of X – rays in crystals, and it would seem that all questions of the influence of these factors on the scattering intensity of X – rays have been thoroughly investigated and clarified. However, new experimental data, such as sectional topograms obtained from a two-block crystalline system with a narrow air gap and from a thick absorbing ideal crystal in the reflection position, show that it is necessary to conduct special studies to elucidate the nature of the influence of the above factors on the intensity of $X-$ray scattering. Therefore, a further more detailed study of these issues is important both for the development of $X-$ray diagnostic studies and for the unambiguous interpretation of $X-$ray diffraction patterns using the interpretation of a section topogram, which the present work is devoted to.

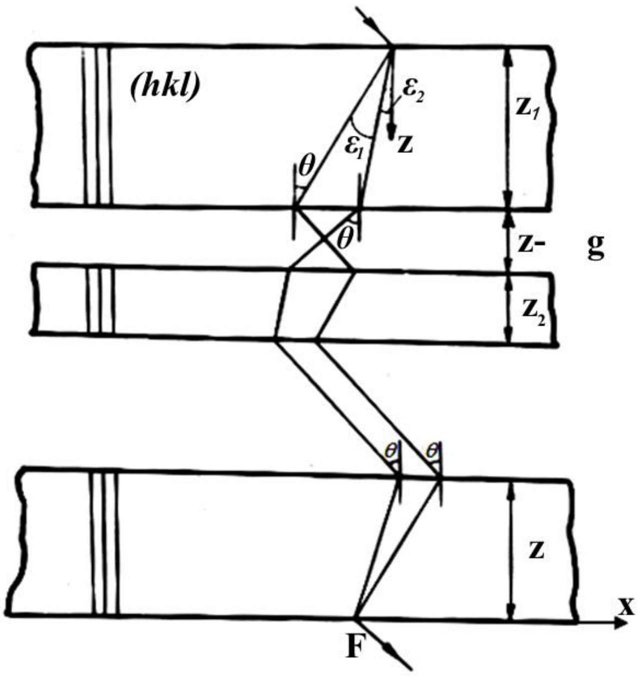

Fig. 1. A system consisting of a two-unit interferometer and a magnifying crystal

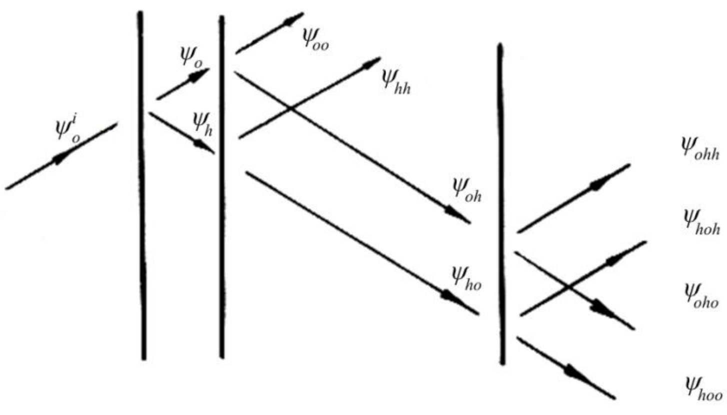

Fig. 2. The components of the amplitude of the incident wave after diffraction in the first, second blocks and in the magnifier block

Obviously, the higher the resolution of the $X-$ray diffraction methods, the greater the visibility of the fine structure of the $X-$ray diffraction patterns, therefore, the more information received from these patterns is about the structural imperfections of crystalline materials.

We, in order to increase the resolution of $X-$ray diffraction methods, propose a new method, which is theoretically proven, and with the help of which we experimentally observed displacement lines, moire bands, pendulum bands and other fine structures of diffraction images that are not observed by conventional methods. So, it is known [10] that, during $X-$ray diffraction in crystals, a strong angular increase in the beam occurs, which is expressed by the formula:

$$M = \frac{d\eta}{d\varepsilon} = \frac{K\cos\theta_B}{R\cos\varepsilon} \tag{1}$$

where $d\varepsilon$ - is the angle of convergence of the incident beam, $d\eta$ -is the angle of divergence of the incident beam in the crystal, θ_B -is the Bragg angle, R -is the radius of the dispersion surface, K -is the wave number $(K = 1/\lambda)$.

As can be seen from (1), a crystal is a powerful magnifier: when $M_0K_{\alpha_1}$ emitting and $(2\bar{2}0)$ reflecting silicon, M has an order of magnitude 10^2. This effect of angular magnification can be used to obtain linear magnification, which makes it possible to increase the resolution of X-ray diffraction patterns, which is the aim of the present work. This goal is achieved by the fact that a beam containing information about structural defects of the studied sample or moire patterns obtained from a two or three-block interferometer is passed through an ideal thick crystal in the reflection position.

Thus, the aim of this work is to study the imperfections of crystalline substances on the basis of revealing the fine structure of $X-$ray diffraction patterns during dynamic $X-$ray scattering, using the interpretation of the obtained sectional topograms.

2. Theoretical Analysis

Let a spatially inhomogeneous wave packet with amplitude Ψ_0^i fall on a crystalline system consisting of a two-block system with a narrow gap and a thick absorbing crystal (Fig. 1). The third block (thick block) is located so far from the first two that the beams diffracted in the first two do not overlap each other on the input surface of this block, i.e. the third block plays the role of a magnifier.

After diffraction in the first crystal, the incident beam is decomposed into two components: the transmitted wave with amplitude after diffraction in the first crystal, the incident beam is decomposed into two components: the transmitted wave with amplitude Ψ_0 and diffracted with amplitude Ψ_h (Fig.2). After diffraction in a two-block system with a narrow gap (after the second block), the beam decomposes into four components with amplitudes Ψ_{h0}, Ψ_{hh}, Ψ_{0h} and Ψ_{00} (Fig.2).

Let us consider the diffraction of waves with amplitudes Ψ_{h0} and Ψ_{0h} in the third thick plate (the beams Ψ_{hh} and Ψ_{00} do not differ from the considered ones in the nature of interference). In the third thick plate, the beams Ψ_{h0} and Ψ_{hh} form four beams, with Ψ_{h00} and Ψ_{0h0} interfering in the direction of reflection, and Ψ_{h0h} and Ψ_{0hh} in the direction of incidence. To find the distribution of interference fringes, we need to know the phase value Φ_q of the interfering beams, which are determined by the expression:

$$\Psi_q = \left|\Psi_q\right| \exp(i\Phi_q)$$

These phases can be easily found from the Takagi equation [11], using the stationary phase method [12,13] and omitting the terms corresponding to strongly absorbed wave modes. In the symmetric Laue case for the phases of the bundles Ψ_{h0h} and Ψ_{0hh} we obtain the following expressions:

$$\begin{aligned} \Psi_{0hh} &= -\frac{\pi}{\Delta_0}(Z+Z_1+Z_2)(1-P_1^2)^{1/2} + \frac{3}{4}\pi \\ \Psi_{h0h} &= -\frac{\pi}{\Delta_0}(Z+Z_1+Z_2)(1-P_2^2)^{1/2} + \frac{3}{4}\pi \end{aligned} \qquad (2)$$

where Δ_0 - is the real part of the extinction length, Z - is the thickness of the thick plate, Z_1 and Z_2 - are the thicknesses of the first and second crystals of the two-crystal system, the parameters $P_1 = tg\varepsilon_1 / tg\theta, P_2 = tg\varepsilon_2 / tg\theta$ characterize the directions of energy fluxes, and θ - is the Bragg angle.

The Ψ_{h00} and Ψ_{0h0} bundles will not be considered, because by the nature of the interference, they are similar with the bundles Ψ_{0hh} and Ψ_{h0h}.

From (2) for the phase difference $\Delta\Phi = \Phi_{0hh} - \Phi_{h0h}$ we obtain

$$\Delta\Phi \approx \frac{\pi}{\Delta_0}(Z+Z_1+Z_2)\frac{PdP}{(1-P^2)^{1/2}}$$

where $P = (P_1+P_2)/2$ and $dP = P_2 - P_1$ calculated for the case of strong absorption, i.e. calculations are made for the central part of the topogram. Interfering rays, which make up the angles ε_1 and ε_2 with the normal of the input surface, satisfy the condition:

$$Z+Z_1+Z_2 = \frac{2Z_g}{dP} = \frac{2Z_g tg\theta}{tg\varepsilon_2 - tg\varepsilon_1}, \qquad (3)$$

where Zg - is the width of the air gap (non-diffracting zone).

Combining the last expression with the condition of the maxima of the interference bands $\Delta\Phi = 2\pi n$ where $n = 1, 2, 3, ...$ you can get the coordinates of the surfaces (bands) of maximum intensity:

$$X_n = \pm \frac{n\Delta_0 tg\theta}{Z_g\left[1+(n\Delta_0/Z_g)^2\right]^{1/2}}(Z+Z_1+Z_2)$$

The direction of the *X* coordinate axis is shown in Fig. 1. In the central part of the topogram, without making a big mistake, we can assume that $(n\Delta_0/Z_g)^4 \ll 1$ then for the period value of these bands we get:

$$\Lambda = \frac{(Z+Z_1+Z_2)\Delta_0 tg\theta}{Z_g}\left[1-\frac{3}{2}n^2\left(\frac{\Delta_0}{Z_g}\right)^3-\frac{3}{2}n\left(\frac{\Delta_0}{Z_g}\right)^3-\frac{1}{2}\left(\frac{\Delta_0}{Z_g}\right)^3\right] \quad (4)$$

Since $Z_g \ll Z_1$ and $Z_g \ll Z_2$, we get a family of parallel planes perpendicular to the scattering plane, the intersection of which with the photographic plate is a family of straight lines [14-17], and the general character of the decay of the period of the bands with an increase in their order n can be noted.

When operating without a thick crystal, displacement bands are obtained with a period

$$\Lambda' = \frac{(Z_1+Z_2)\Delta_0 tg\theta}{Z_g}\left[1-\frac{3}{2}n^2\left(\frac{\Delta_0}{Z_g}\right)^3-\frac{3}{2}n\left(\frac{\Delta_0}{Z_g}\right)^3-\frac{1}{2}\left(\frac{\Delta_0}{Z_g}\right)^3\right] \quad (5)$$

Comparing the values of periods (4) and (5), we can conclude that the presence of a magnifying crystal makes it possible to obtain interference fringes with the following linear increase coefficient in the direction of the diffraction vector:

$$D = 1 + \frac{Z}{Z_1+Z_2} \quad (6)$$

This increase is interference in nature and, as can be seen, depends on the thickness of the thick plate. When choosing a rather large value of Z, one can achieve an increase of up to 10 or more times and observe experimentally interference fringes with a large period and resolution. However, an excessive increase in the thickness of a thick plate is impractical because with increasing thickness, absorption increases and the intensity of reflected beams decreases.

3. Experimental Part

To confirm the validity of the above reasoning, experimental studies were carried out using a highly perfect single-crystal two-block system with a narrow air gap and from a thick absorbing ideal crystal in the reflection position (Fig.3).

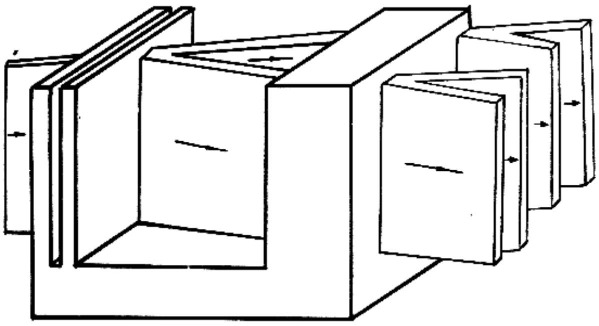

Fig. 3. A system consisting of two thin, closely spaced blocks and a magnifying block

Thickness of thin blocks of a two-crystal system $Z_1 = 420\mu m,$ $Z_2 = 1315\mu m$ a thick perfect crystal $Z = 5550\mu m$ width of a non-diffracting zone $Z_g = 290\mu m$ radiation $M_0K_{\alpha_1}$, reflection $(2\bar{2}0)$, width of a collimated beam $80\mu m$.

The system shown in fig. 3 is schematically shown in fig. 4, where a narrow $X-$ray beam, passing through a collimator with a diaphragm, falls on a two-block system consisting of crystals 1 and 2. The diffracted beam falls on a perfect thick crystal 3, which is in the reflection position, and the transmitted beam is delayed by the screen 4. The diffracted beam containing moire patterns, passes through a thick crystal, which without changing the character of moire, increases this moire pattern. In fig. 4a shows a moire pattern formed by a dual-crystal system.

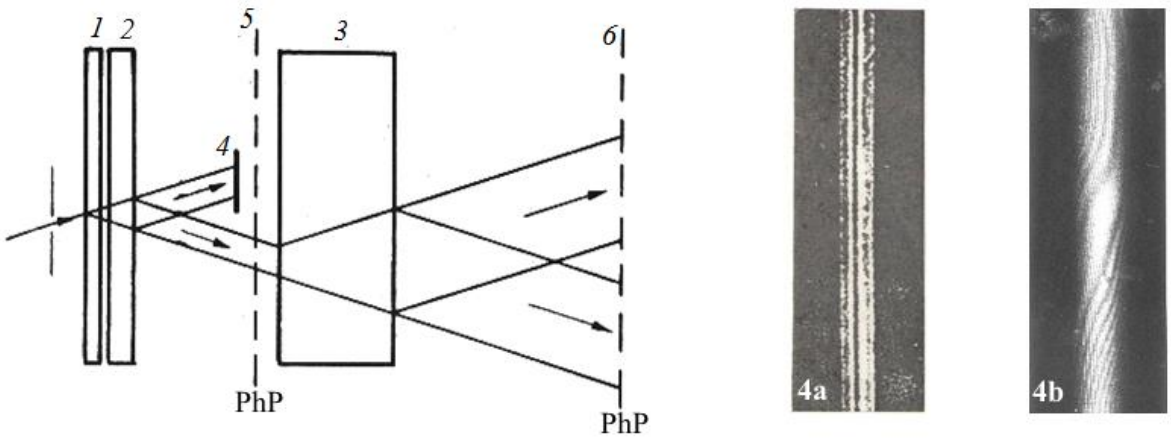

Fig. 4. An increase in X-ray moire patterns obtained using a dual-crystal system. 4a moire pattern formed by a dual-crystal system; 4b — moiré pattern 4a after enlargement

This image was obtained on a photographic plate 5 placed between the second and third blocks (Fig. 4). In fig. 4b shows the same moire pattern on film 6, located after the third block. As can be seen from these figures, after the second block, the moire on the film is almost invisible, and only after the third block, i.e. after enlargement, moire stripes are clearly visible.

4. Results and its Discussion

In a similar way, one can obtain an increase in interference patterns obtained from interferometers of an arbitrary type, and also increase the resolution of $X-$ray topographic methods.

This effect can be applied in areas of physical research, such as $X-$ray diffraction of microdefects, $X-$ray spectroscopy, $X-$ray interferometry, precision $X-$ray diffraction analysis, and also for studies of the fine structure of interference patterns.

It may seem that the interference patterns observed after the magnifier (an ideal thick crystal) did not exist before it and formed in it, that is, the last crystal does not play the role of the magnifier, but participates in the formation of these patterns. The fact that the last thick crystal only increases the linear dimensions of the diffraction pattern and does not introduce any additional information into the interference pattern can be verified on the basis of the following theoretical considerations (reasoning) and experimental facts:

1) The magnifying crystal is thick and ideal, therefore, the field having a large absorption coefficient completely disappears, and inside the crystal the distribution of the field having a period equal to the interplanar distance of the reflecting planes is not stored outside the crystal. Further, since the magnifier crystal is perfect and defects are not observed on its topogram, it follows from what was said in this section that the magnifier crystal does not change the nature of the intensity distribution in the beam passing through it.
2) It can be seen from Figs. 4a and 4b that, after thin plates, the interference pattern is not observed (Fig. 4a), but after a thick crystal it is observed (Fig. 4b), and the primary moire pattern (Fig. 4a) and its enlarged pattern (Fig. 4b) differ only in dimensions in the scattering plane.
3) We can verify that this interference pattern is not created by a thick crystal, but by the superposition of waves on the second crystal obtained in the first thin crystal as a result of splitting of the primary wave. Indeed, if one of these thin plates is removed or the distance between them is increased, then the interference pattern observed after the thick crystal disappears. Consequently, the interference pattern observed after the thick crystal arose in the subsystem of two thin crystals and became visible after magnification.

5. Conclusion

The results of our research form the basis for stating the following:

1. The crystal-magnifier does not introduce new information into the interference pattern, but only increases its angular dimensions in the scattering plane.
2. The magnifier crystal does not change the nature of the intensity distribution in the beam passing through it.
3. The crystal-magnifier reduces the overall intensity without changing the interference pattern.

4. An increase in D depends on the relative thicknesses of the magnifier Z and the total thickness of the thin plates $(Z_1 + Z_2)$: with an increase in Z and a decrease in the sum of $(Z_1 + Z_2)$, this parameter increases.
5. With an increase in the sum $(Z_1 + Z_2)$, the magnification in the thick crystal D decreases and tends to unity, i.e., the thick crystal ceases to play the role of a magnifier. But, as expression (6) shows, for large Z_1 and Z_2, the interference pattern is increased by these plates themselves and the need for an additional magnifier disappears.

Acknowledgments

This work was supported by the RA MES Science Committee, in the frames of the research project №18T-1C395

Conflicts of interest

There is no conflict of interest.

Author Contributions

Authors H.G. Margaryan, invented and developed the experiment; authors H.R. Drmeyan participated in data processing and carried out theoretical calculations.

References

[1] M. Tolan, G. Vacca, S.K. Sinha et al., J. Phys. D., V.28, P. A231, (1995)
[2] A.H. Aboyan, Thes. doc. RSNE-99, Moscow: IR RAS, p.172. (1999) (in Russian)
[3] B. Caderstrom, Cahn R., N. Danielsson et al., Nature, V.404. pp 951-955, (2000)
[4] Aristov V., Grigoriev M., Kuznetsov S. et al., Appl. Phys. Lett., V.77., pp 4058-4063, (2000)
[5] V.A. Bushuev, R.M. Imamov, E.Kh. Mukhamedzhanov, A.P. Oreshko, Crystallography, V. 46, No. 6, pp. 991-997, (2001) (in Russian)
[6] H.R. Drmeyan, A.H. Melkonyan and Z.H. Knyazyan, Journal of surface Investigation X-ray, Synchrotron and Neutron Technigues, Vol.11, №5, pp 1089-1095, (2017) (in Russian)
[7] H.R. Drymeyan, Surface. X-ray, synchrotron and neutron studies, No. 4, p.103-106, (2018)
[8] V.R. Kocharyan, A.E. Movsisyan and A.S. Grogolev, Journal of Contemporary Physics (Armenian Akademy of Sciances), Vol.53, №3, pp 263-269, (2018)
[9] T. Takeda, A. Momose, Q. Yu, J. Wu, K. Hirano, Y. Itaia, J. Synchr. Rad. V.7, pp 280-286, (2000)
[10] A. Authier, Acta geologica et geografhica Universitatis Comenianac. Geologica, 14, 37 (1968).
[11] S. Takadi Acta Cryst, 15, 1311 (1962), J. Phys. Soc. Japan 26, 1239 (1969).
[12] M. Bourne, E. Wolf, "Fundamentals of Optics." Publishing House “Science’’, M. (1970) (in Russian)
[13] A.G. Sveshnikov, A.N. Tikhonov, “The theory of a function of a complex variable”, M. Nauka. 304 p. (1967) (in Russian)
[14] A. Authier, A.D. Miln, M. Sauvage, Phys. Stat. Sol., V. 26, pp 469-484, (1968)
[15] M. Hart, A.D. Milne, Acta Cryst., A26, pp. 223-229, (1970)
[16] H. Hashizume, H. Ishida, K. Kohra, Phys. Stat. sol. (a), 12, 453, (1972)
[17] S. Tanemura, A.R.Lang, Z. Naturforsch, V. 28a, pp. 668-676, (1973)